Springer

KSME

Journal of Mechanical Science and Technology 24 (9) (2010) 1829~1837
www.springerlink.com/content/1738-494x
DOI 10.1007/s12206-010-0607-x

An experimental evaluation of pre-yield and post-yield rheological models of magnetic field dependent smart materials †

N. Mohammadi[1], M. J. Mahjoob[1,*] B. Kaffashi[2] and S. Malakooti[1]

[1]*NVA Research Centre, School of Mechanical Engineering, University of Tehran, Iran*
[2]*School of Chemical Engineering, University of Tehran, Iran*

(Manuscript Received June 21, 2009; Revised April 8, 2010; Accepted April 26, 2010)

Abstract

The rheological behavior of field-dependent smart fluids in both the pre-yield and post-yield regimes is investigated. Typical viscoelastic and viscoplastic models are employed to model the fluids behavior. Viscoelastic models are used widely in the pre-yield regime. Viscoplastic models are also used extensively in both the pre-yield and post-yield regimes. Two smart fluids including a ferromagnetic nano-particle fluid and an MR fluid are examined here. Using an MCR300 rheometer, the rheological properties of the fluids in both oscillation and rotational mode are measured. In the oscillation mode, the storage and loss moduli versus frequency are measured. In the rotational mode, shear stress, shear rate, viscosity and torque are measured. In the frequency domain, the pre-yield behavior of the ferromagnetic nano-particle fluid is modeled by Kelvin-Voigt solid model. Also, the three-parameter fluid model is used to model the pre-yield behavior of the MR fluid. Two viscoplastic models including Bingham-plastic and Herschel-Bulkley models are selected to model the rheological behavior of fluids in the time domain. Which model is more appropriate depends on the external magnetic field and the shear rate. Both models are used here to model the fluids' behavior. The models properly predict the results observed in the experiments.

Keywords: Smart materials; MR fluids; Ferromagnetic fluids; Viscoelastic models; Viscoplastic models

1. Introduction

EMR (electrorheological/magnetorheological) fluids are a group of smart materials whose material properties can be controlled by applying an external electric/magnetic field. When an external field is applied to the EMR fluids, substantial changes occur in rheological, magnetical, electrical, thermal, optical and acoustic properties of the fluid. Of the change in rheological properties of the fluid, in particular, the most important effect of the field is the enhancement of the fluid resistance to flow. As the field strength goes up, the viscosity of the fluid increases and its structure changes from a fluid to a solid-like material. This change in the structure and in the rheological properties occurs in a very short time, that is, lower than a few milliseconds. The response of these fluids to the field is continuous, fast and reversible. The fluid structure and material properties return to the initial state once the field is removed or a shear stress higher than yield stress is exerted onto the fluid. The yield stress depends on the field strength and the fluid composition. Using nano-particles (vs. micron-scale particles) with constant weight ratio improves the stability of fluid against settlement. However, it adversely affects the fluid performance by decreasing the yield stress [1].

EMR fluids are classified into ER, MR and ferromagnetic fluids. These fluids are mainly a composition of some particles suspended in a carrier (base) liquid. The rheological properties of such fluids depend on variables such as particle density, particle size, shape of the particles and their distribution, carrier fluid properties, additives, external field and temperature. Once the fluid is subjected to a field, the particles are aligned across the field creating a chain-like structure. The new structure alters the shear resistance and viscosity of the fluid [2]. A significant property of EMR fluids is the dependence of their yield stress on the external field. When the shear stress increases and reaches the critical value, yield stress, the material flows and then behaves close to a Newtonian fluid [3]. The EMR fluids' behavior in two regimes including the pre-yield and post-yield is studied independently. Although the fluids' behavior in the post-yield regime is simple, their behavior in the pre-yield regime is complex [3].

Several models have been presented to characterize the pre-yield behavior of EMR fluids. No specific model, however, could properly describe the pre-yield behavior of all EMR fluids. In general, viscoelastic models are extensively used in the pre-yield regime to model the rheology of the EMR fluids. These models are comprised of elastic springs and viscous

† This paper was recommended for publication in revised form by Associate Editor Seong Beon Lee
*Corresponding author. Tel.: +98 21 8800 5677, Fax: +98 21 8801 3029
E-mail address: mmahjoob@ut.ac.ir

dashpot elements [3]. Model parameters such as spring constants and damping coefficients are determined through rheology tests. Classification of the viscoelastic models is done according to fluid-like or solid-like behavior of the viscoelastic material. The common fluid-like viscoelastic models are viscous dashpot [4, 5], Maxwell fluid [6, 7], and three-parameter fluid [8, 9]. Elastic spring [10, 11], Kelvin-Voigt solid [12-14], and three-parameter solid [15] are the common solid-like viscoelastic models. Viscoplastic models are widely used to model the entire pre-yield and post-yield behavior of the EMR fluids. The fluid behavior under field is nonlinear and different in the pre-yield and post-yield regimes [1]. In the pre-yield regime, the fluid resists against flowing; therefore, in this regime the behavior of the fluid is similar to solid. The fluid flows when shear stress passes the yield stress.

Two simple viscoplastic models are commonly used: the Bingham-plastic and Herschel-Bulkley. In these models, two parameters, including the yield stress and the viscosity, are used to describe the behavior of the fluid. Where shear stress is proportional to the shear rate within the post-yield regime (i.e., constant viscosity), the model is Bingham-plastic. Once the material behaves such that the viscosity is not constant, the Herschel-Bulkley viscoplastic model is a better choice than the Bingham-plastic model [1].

In this paper, two EMR fluids, a ferromagnetic nano-particle fluid and an MR fluid, are examined. First, the common viscoelastic and viscoplastic models are reviewed. Then, using experimental results of the rheology tests, the proper models which best describe the rheological behavior of these fluids (in both the pre-yield and post-yield regimes) are presented. From experimental results, the Kelvin-Voigt solid model is used to describe the rheological behavior of the ferromagnetic nano-particle fluid in the pre-yield regime. In addition, the three-parameter fluid is employed to model the rheological behavior of the MR fluid in the pre-yield regime. In the time domain, the Bingham-plastic and Herschel-Bulkley viscoplastic models are used to determine the rheological behavior of the fluids, in the entire pre-yield and post-yield regimes. A specific viscoplastic model is preferred depending upon the field strength and the shear rate.

The models describing the dependence of the shear modulus and yield stress on the magnetic field are also investigated. The experimental results support the existing models, which formulate these variations by quadratic polynomials.

2. Theory

2.1 Viscoelastic models

The common viscoelastic models are illustrated schematically in Fig. 1. Models are classified according to solid-like or fluid-like behavior of the fluids. These models include two basic components, viscous dashpot and elastic spring. Complex viscoelastic models are composed of several dashpots and spring elements. Based on the rheological tests, the pre-

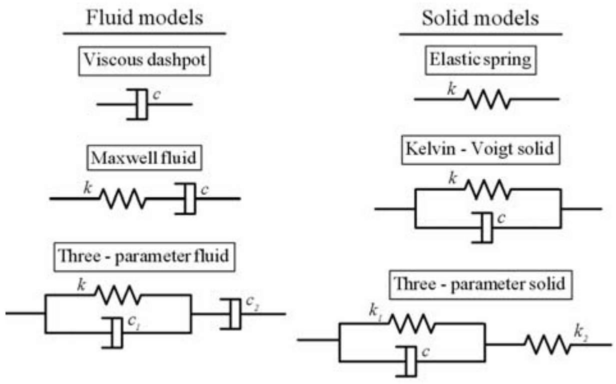

Fig. 1. Common viscoelastic models for rheological modeling of the EMR fluids.

yield behavior of the EMR fluids may be described by a number of viscoelastic models.

Generally, viscoelastic models are specified in frequency domain by defining a complex modulus. The real part of this modulus shows the stiffness properties of the material, namely the elastic or storage modulus, and the imaginary part indicates the damping properties of material, namely viscous or loss modulus. These components comprise the response (deformation or strain) characteristics of a viscoelastic material to an external input (force or stress). Hence,

$$\begin{aligned} &\gamma = \gamma_0 \sin \omega t \\ &\tau = G'\gamma_0 \sin \omega t + G''\gamma_0 \cos \omega t \\ &G^* = G' + \mathrm{j}G'' \end{aligned} \quad (1)$$

where γ refers to the shear strain, and G^*, G' and G'' indicate the complex modulus, storage (elastic) modulus and loss modulus, respectively. From the rheology test results in the frequency domain, the storage and loss moduli versus frequency are determined.

For a purely viscous element (dashpot), the storage modulus is zero and the loss modulus increases linearly with frequency; therefore, the storage and the loss modulus are given as follows:

$$G' = 0 \ , \ G'' = c\omega \quad (2)$$

where c indicates the dashpot constant. For the Maxwell fluid, the relations between the model parameters and the storage and loss moduli are given by:

$$G' = \frac{k(c\omega)^2}{k^2 + (c\omega)^2} \ , \ G'' = \frac{k^2 c\omega}{k^2 + (c\omega)^2} \quad (3)$$

where k refers to the spring constant. However, for a three-parameter fluid:

$$G' = \frac{k(c_2\omega)^2}{k^2 + \left[(c_1 + c_2)\omega\right]^2} \ , \ G'' = \frac{\left[k^2 + (c_1 + c_2)c_1\omega^2\right]c_2\omega}{k^2 + \left[(c_1 + c_2)\omega\right]^2} \quad (4)$$

Similar relations can be derived for the solid-like models. In contrast to the fluid models, for the elastic spring, the storage modulus is independent of frequency and the loss modulus is zero:

$$G' = k \ , \ G'' = 0 \tag{5}$$

For a Kelvin-Voigt solid model, the storage modulus is independent of frequency while the loss modulus increases linearly with frequency. The relations between the model parameters and storage and loss moduli are then:

$$G' = k \ , \ G'' = c\omega \tag{6}$$

The three-parameter solid is characterized by:

$$G' = \frac{k_2\left[(k_1+k_2)k_1 + (c\omega)^2\right]}{(k_1+k_2)^2 + (c\omega)^2} \ , \ G'' = \frac{k_2^2 c\omega}{(k_1+k_2)^2 + (c\omega)^2} \tag{7}$$

Experimental results obtained in the rheology tests are generally compared with the graphs representing the viscoelastic models [7, 8] to arrive at a suitable model for material behavior.

2.2 Viscoplastic models

Herein, two common viscoplastic models including the Bingham-plastic (BP) and Herschel-Bulkley (HB) are examined. In viscoplastic models, the fluid behavior in both pre-yield and post-yield regimes is considered. The boundary between these two regimes is specified by the critical shear stress (yield stress). In the pre-yield regime where shear stress is lower than yield stress, the behavior is assumed as a solid. The material flows after the shear stress passes over the yield stress.

In the BP model, the difference between shear stress and yield stress (in the post-yield region) equals the shear rate multiplied by fluid viscosity [1]. The shear stress-shear rate relation for the BP model is therefore written as:

$$\tau = \tau_y + \eta\dot{\gamma} \tag{8}$$

in which τ_y is the yield stress, η the fluid viscosity and $\dot{\gamma}$ the shear rate.

In the HB model, the rheological behavior of fluid is the same as BP model in the pre-yield region. Here, the difference between shear stress and yield stress is equal to the consistency factor multiplied by some power of the shear rate [1]. The shear stress-shear rate relation is then given by:

$$\tau = \tau_y + \bar{k}\dot{\gamma}^m \tag{9}$$

where $\bar{k}$ indicates the consistency factor and m is the flow index. The post-yield behavior of flow is classified according to the flow index values. When the flow index is greater than $1\ (m>1)$, the fluid behavior is shear thickening.

Fig. 2. MCR300 rheometer used for rheological measurement under magnetic field.

Once the flow index is lower than $1\ (m<1)$, the fluid behavior is shear thinning. At $m=1$, the fluid behavior is similar to the BP model.

Experiments are conducted here for two types of fluids, for which appropriate viscoplastic models are then derived based on the rheology test results.

3. Experimental work

3.1 Test apparatus

A Paar Physica MCR300 rheometer (see Fig. 2) is used to measure the rheological specifications of the fluids. The rheometer is an air bearing type rheometer. The necessary air is supplied by a 250-lit tank. Air passes through a series of filters absorbing its moisture and oil contaminants. The pure, clean and dry air flows into the rheometer at 5 bar and 110 lit/min. The chosen geometry is parallel plate. There is a 1-mm gap between the plates. The lower plate is fixed and the upper one rotates. A magnetic cell is utilized to apply the required continuous magnetic field. In addition, a water-based heater/cooler system is used to provide a uniform constant temperature. This system is capable of adjusting the fluid temperature at values between -30 ^{o}C and 180 ^{o}C. All the measurements are performed at 25 ^{o}C.

3.2 Measurement

Here, two EMR fluids including a ferromagnetic nanoparticle fluid (named NMF-128DV synthesized in Iran Color Research Center) and an MR fluid (named MRHCCS4-A made by U.K. LIQUID RESEARCH Company) are used. Fluid specifications are in Tables 1 and 2. Rheological properties are measured in both the time (rotational mode) and frequency domains (oscillation mode).

3.2.1 Rotational mode

In this measurement mode, shear stress, shear rate, viscosity

Table 1. Specifications of the ferromagnetic nano-particle fluid.

Base fluid	Operating temperature	Density	Color	Particles	Particles size	Particles volume ratio
Hydrocarbon	-20 (ºC) to 120 (ºC)	1.2 (g.cm^{-3})	Black	Magnetite	14 (nm)	6.5 %

Table 2. Specifications of the MR fluid.

Base fluid	Operating temperature	Density	Color	Particles packing (wt)
Hydrocarbon	-40 (ºC) to 140 (ºC)	2.49 (g.cm^{-3})	Gray	70 %

and torque are measured at steady-state conditions. First, using a time transient test, the required time after which the fluid becomes steady is determined. This time depends on the fluid properties and external magnetic field. When the fluid is subjected to an external field the time constant increases. The range of time constants in our tests is from 10 to 100 seconds. First, a sufficient volume of the fluid (approximately 0.2 ml) is placed in between the rheometer plates. Then the upper plate rotates while a sensor measures torque and the related external force. The shear rate range is from 0.1 to 1000 1/s. The upper limit of the shear rate is chosen such that the fluid does not leave a gap between the two plates. Thirty test points are measured for each fluid sample. The time duration of each measurement is three seconds and the total time of each fluid sample test is ninety seconds. For the ferromagnetic nano-particle fluid, the range of the external magnetic fields experienced here corresponds to 0 to 1 A current. In fact, the fluid fails above 1 A. However, the applicable range for the other fluid (MR fluid) is 0 to 2 A.

3.2.2 Oscillation mode

In this measurement mode, the fluid is subjected to an oscillatory force at different frequencies. The frequency is varied from 0.01 to 100 Hz. In this mode, the storage and loss moduli versus frequency are calculated. First, using amplitude sweep test, the storage and loss moduli versus shear stress are measured at constant frequency. The aim of this test is to determine the maximum shear stress related to linear behavior of the fluid. Then, using frequency sweep test, the storage and loss moduli versus frequency are measured. The frequency sweep test includes two modes: constant shear rate (CSR) and constant shear stress (CSS). The MCR rheometers measurement is based on applying shear stress to the fluid. Therefore, we used the CSS mode in the oscillation test. In the CSS mode, the fluid is subjected to a constant shear stress (the maximum shear stress associated with the amplitude sweep test) and the storage and loss moduli versus frequency are measured. Here, similar to the rotation mode, the range of the fields applied to the ferromagnetic nano-particle fluid and the MR fluid is 0 to 1 A and 0 to 2 A, respectively.

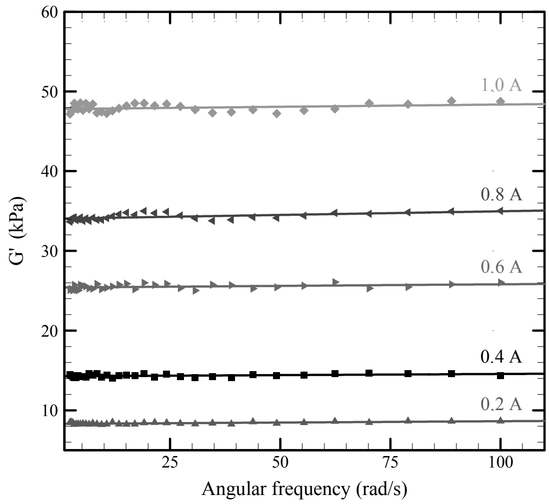

Fig. 3. Storage modulus vs. frequency in different magnetic fields (0.2-1 A) for ferromagnetic nano-particle fluid (model: curve-line, test: discrete marks).

4. Rheology test results and modeling

4.1 Modeling in frequency domain

Both the test and model values for storage and loss moduli versus frequency are shown in Figs. 3 to 6. The model (s) used to generate the curves in these figures will be discussed later in the next section. Least square method in conjunction with Levenberg-Marquardt algorithm is used to find the parameters of the models.

The relation between the field strength and the shear-storage modulus can also be investigated. This relationship has been described as [16]:

$$G' \approx 3\phi\mu_0 M_s \mathrm{H} \tag{10}$$

in which ϕ is the volume fraction of the suspended particles of the fluid, μ_0 is the permeability of the free space, M_s is the saturation magnetization of the particle and H (A m^{-1}) is the strength of external field. At low magnetic fields (i.e., lower than 0.6 T), where M_s is expected to be linearly related to H, Eq. (10) is expressed as follows [17]:

$$G' \propto \phi\mu_0 \mathrm{H}^2 \tag{11}$$

Eq. (11) shows a square power relationship between shear-storage modulus and magnetic field strength. Therefore, a quadratic polynomial is fitted to the experimental values of shear-storage modulus of the fluids versus field strength. The details of these relationships for the specific fluids under study are presented in sections 4.1.1 and 4.1.2.

4.1.1 Ferromagnetic nano-particle fluid

Fig. 3 shows that variations of storage modulus vs. frequency are small at different magnetic fields. The results in Fig. 4 also imply that the loss modulus has low variation with

Table 3. Kelvin-Voigt model parameters: spring constant and damping coefficient (ferromagnetic nano-particle fluid).

I (A)	0.2	0.4	0.6	0.8	1
k (kPa)	8.462	14.425	25.631	34.549	48.053
c (Pa.s)	2.821	6.574	10.812	4.673	5.706

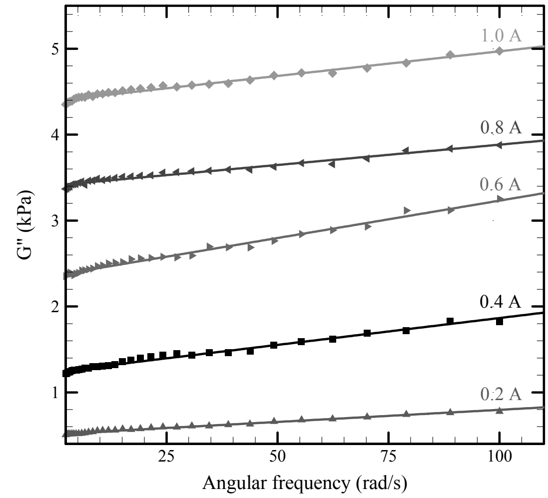

Fig. 4. Loss modulus vs. frequency in different magnetic fields (0.2-1 A) for ferromagnetic nano-particle fluid (model: curve-line, test: discrete marks).

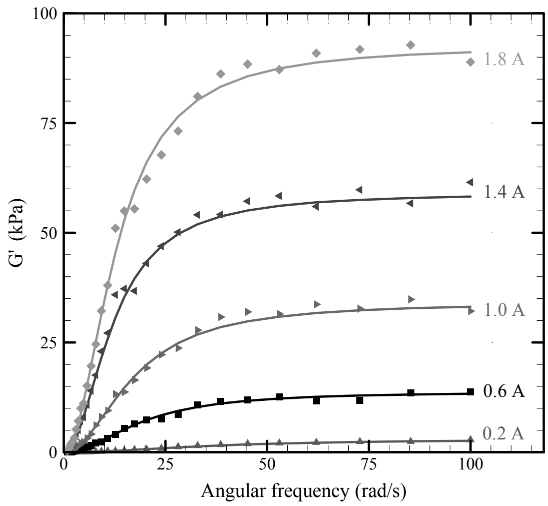

Fig. 5. Storage modulus vs. frequency in different magnetic fields (0.2-1.8 A) for MR fluid (model: curve-line, test: discrete marks).

frequency. However, the loss modulus is considerably smaller than the storage modulus. The variations follow the same trend in different fields. Therefore, the pre-yield behavior of the fluid is modeled by the Kelvin-Voigt solid model. The parameters of the model including spring constant and damping coefficient are presented in Table 3. For comparison, the test results together with the model results are shown in Figs. 3 and 4. Based on the model discussed at the end of the previous section, the relation between field and shear modulus can now be evaluated. The polynomials representing the shear-

Table 4. Three-parameter model: spring constant and damping coefficients (MR fluid).

I (A)	0.2	0.4	0.6	0.8	1	1.2	1.4	1.6	1.8	2
k (kPa)	5.25	10.37	21.27	32.43	47.32	59.26	73.24	87.93	112.34	132.33
c_1 (Pa.s)	36	112	215	332	415	547	608	659	798	874
c_2 (kPa.s)	0.107	0.421	0.893	1.67	2.34	3.87	5.38	6.54	7.89	8.93

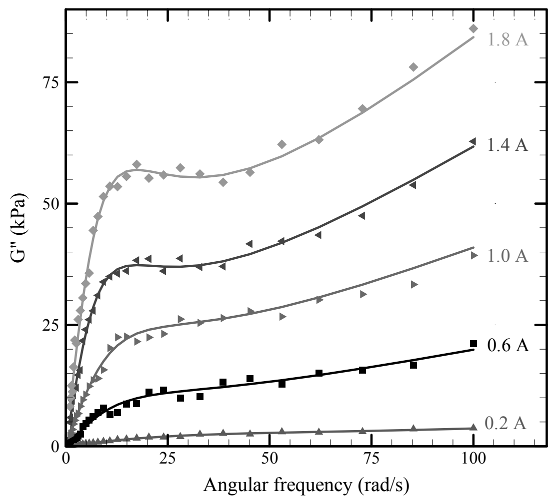

Fig. 6. Loss modulus vs. frequency in different magnetic fields (0.2-1.8 A) for MR fluid (model: curve-line, test: discrete marks).

storage modulus of the NMF material in different magnetic fields (in terms of current 'I' in Amps or field 'H' in kAm^{-1}) were computed as follows:

$$G'(\text{Pa}) = 2.36\times10^{4}\text{I}^{2} + 2.09\times10^{4}\text{I} + 3.03\times10^{3}$$
$$G'(\text{Pa}) = 0.6364\ \text{H}^{2} + 97.78\ \text{H} + 4.187\times10^{3} \quad (12)$$

It should be noted that these relations are only developed for the regions where the storage modulus no longer depends on frequency ($\omega > 7$ rad/s in Fig. 3, for instance). In fact, such relationships cannot be offered, in particular, for loss modulus of the fluid; there is no value of magnetic field for which the loss modulus is independent of frequency (Fig. 4).

4.1.2 MR fluid

Based on the results indicated in Figs. 5 and 6, the pre-yield behavior of the MR fluid is modeled by the three-parameter fluid model. Presented in Table 4 are the model parameters comprising the spring constant and the loss coefficients.

In Figs. 7 to 9, the storage and loss moduli in three values of magnetic field (0.2 A, 1 A and 1.8 A) are shown. The fluid viscous or elastic appearance varies in different fields and frequencies, and the pre-yield behavior of the MR fluid is appropriately modeled by the viscoelastic three-parameter fluid. For $\text{I} < 0.6$ A , the viscous property is more pronounced, than the elastic property, over the entire frequency range. For $0.8 < \text{I} < 1.4$ A , the frequency is an essential parameter to determine which of the viscous or elastic proper-

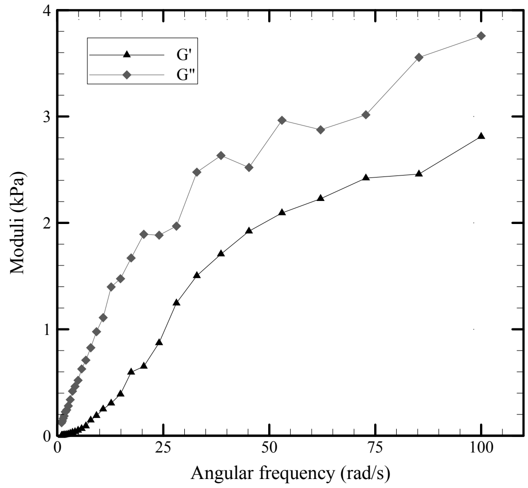

Fig. 7. Measured values of the storage and loss modulus moduli vs. frequency for the MR fluid subjected to 0.2 A external magnetic field.

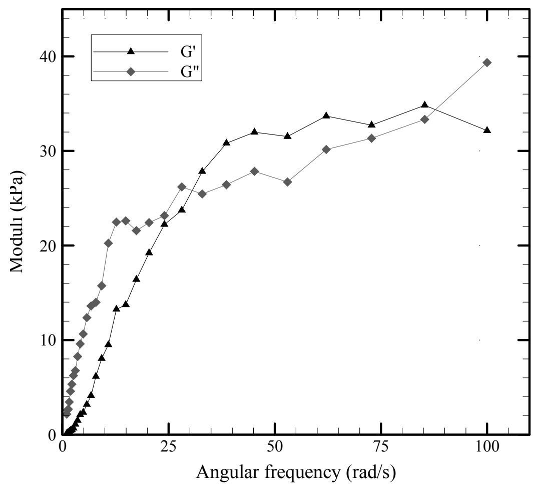

Fig. 8. Measured values of the storage and loss modulus moduli vs. frequency for the MR fluid subjected to 1.0 A external magnetic field.

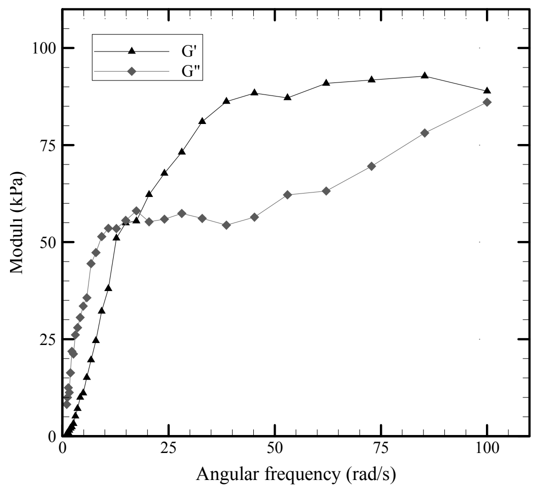

Fig. 9. Measured values of the storage and loss modulus moduli vs. frequency for the MR fluid subjected to 1.8 A external magnetic field.

ties dominates. Here, at medium frequencies the elastic behavior appears stronger than viscous, and vice versa for other frequencies. For $\mathrm{I} > 1.6\ \mathrm{A}$ and for a wide range of frequencies, particularly at medium and high frequencies, the elastic property is stronger than viscous. The viscous effect dominates over the elastic at low frequencies.

Similarly, based on the experimental data, the shear-storage modulus of the MR material corresponding to the different magnetic fields ('H' in kAm^{-1} or current 'I' in Amps) fit the model represented by the following equations:

$$\begin{aligned} G'(\mathrm{Pa}) &= 1.87\times10^4\,\mathrm{I}^2 + 1.55\times10^4\,\mathrm{I} - 3.16\times10^3 \\ G'(\mathrm{Pa}) &= 0.5922\ \mathrm{H}^2 + 48.61\ \mathrm{H} - 1.104\times10^3 \end{aligned} \tag{13}$$

It should be noted that these relations are only developed for the regions where the storage modulus no longer depends on frequency ($\omega > 50$ rad/s in Fig. 5, for instance). Equation (13) reconfirms the accuracy of relations discussed earlier (section 4.1 and references [16-18]) for modeling the field dependency of the shear modulus in MR fluids.

4.1.3 Observations

The fluids' behavior observed above (in sections 4.1.1 and 4.1.2) can be explained as follows.

EMR materials show a gel-like behavior when stronger fields make the structure three-dimensional (3D). As the solid-like behavior develops, there is no viscosity to damp the oscillations energy, i.e., stress and strain are almost in-phase. The magnetic nano-particle fluids should develop a larger 3D structure than MR fluids due to existence of nanoparticles, which form stiffer and larger clusters.

One could see (section 4.1.1) a large difference between storage modulus (G') and loss modulus (G'') where storage modulus is considerably higher than loss modulus. This is probably due to the formation of a 3D particle structure of magnetic nanoparticles forming clusters, caused by a magnetic field. The strength of the structure (elasticity) and, hence, the storage modulus is increased with the strength of the magnetic field. The fact that G' does not change with frequency is due to the formation of a solid 3D structure where there is no dangling part in the structure, which could be dependent upon the frequency, in which case frequency variation would not affect storage modulus.

The amount of current has a direct influence on the structure of MR fluid (section 4.1.2). At small current, i.e., $\mathrm{I} < 0.6\ \mathrm{A}$, the structure is damping energy and is viscous: $G'' > G'$. At such currents (low currents), G' and G'' are more dependent upon frequency at smaller frequencies. This indicates the existence of dangling units' damping energy which makes G'' greater than G'. When $0.8 < \mathrm{I} < 1.4\ \mathrm{A}$, the behavior is viscoelastic, viscous at medium frequencies and elastic at higher frequencies. At $\mathrm{I} > 1.6\ \mathrm{A}$, the MR fluid develops a three-dimensional particle structure and the elastic properties prevail.

Table 5. The BP model parameters for ferromagnetic nano-particle fluid.

I (A)	0.2	0.4	0.6	0.8	1
τ_y (Pa)	192	286	328	352	372
η (Pa.s)	0.1028	0.1363	0.1668	0.1726	0.1752

Table 6. The BP model parameters for MR fluid.

I (A)	0.2	0.4	0.6	0.8	1	1.2	1.4	1.6	1.8	2
τ_y (kPa)	2.023	4.919	8.327	11.73	15.03	17.29	20.88	23.66	25.74	28.36
η (Pa.s)	0.7024	1.397	1.961	2.523	3.075	3.371	3.722	2.762	2.724	2.854

Table 7. The HB model parameters (ferromagnetic nano-particle fluid).

I (A)	0.2	0.4	0.6	0.8	1
τ_y (Pa)	147	210	243	259	261
$\bar{k}$	4.603	8.835	10.26	13.58	22.04
m	0.496	0.456	0.458	0.424	0.362

Table 8. The HB model parameters (MR fluid).

I (A)	0.2	0.4	0.6	0.8	1	1.2	1.4	1.6	1.8	2
τ_y (kPa)	0.4071	1.011	1.375	2.297	3.276	3.990	5.963	6.451	7.418	9.075
$\bar{k}$	597.8	1108	1772	2061	2098	2127	1905	2046	1748	1541
m	0.196	0.235	0.247	0.271	0.303	0.318	0.352	0.353	0.386	0.412

4.2 Modeling in time domain

The variation of shear stress versus shear rate in different magnetic fields is shown in Figs. 10 and 11. The curves here in the figures represent the model (s), which will be discussed later in this section. As it is observed (in Figs. 10 and 11), when the fluids are subjected to an external magnetic field, their behavior is non-linear; the pre-yield and post-yield regimes behave differently. The yield stress changes (increases) with the field strength. A simple model to characterize the fluid rheology is the BP model. The model parameters are the yield stress and viscosity (a constant in the post-yield regime). In cases where the viscosity increases or decreases with shear rate, the HB model is more suitable than the BP model. Both models are examined here.

In Tables 5 and 6, the BP model parameters including the yield stress and viscosity are presented. For the ferromagnetic nano-particle fluid, the yield stress varies from 192 Pa at 0.2 A to 372 Pa at 1 A. The yield stress variation is smooth: monotonically increasing with the field strength. The viscosity of the fluid also increases with magnetic field and approaches the saturation threshold at 0.8 A. In the case of MR fluid, the yield stress varies from 2.023 kPa at 0.2 A up to 28.36 kPa at 2 A. Yield stress varies with the magnetic field smoothly. The viscosity increases up to a threshold at 1.6 A.

The HB model parameters, including yield stress, consistency factor, and flow index, are presented in Tables 7 and 8. Variation of model parameters versus the field is nearly smooth. The yield stress and the consistency factor of the fluids also increase as the magnetic field increases. For the ferromagnetic nano-particle fluid, the yield stress changes from 147 Pa at 0.2 A to 261 Pa at 1 A, and for the MR fluid, the yield stress varies from 407.1 Pa at 0.2 A to 9.075 kPa at 2 A. In this model, the yield stresses of the fluids are greater than the values obtained in the BP model. The flow indexes of the fluids are lower than unity; therefore, the fluids' behavior in the post-yield regime is shear thinning.

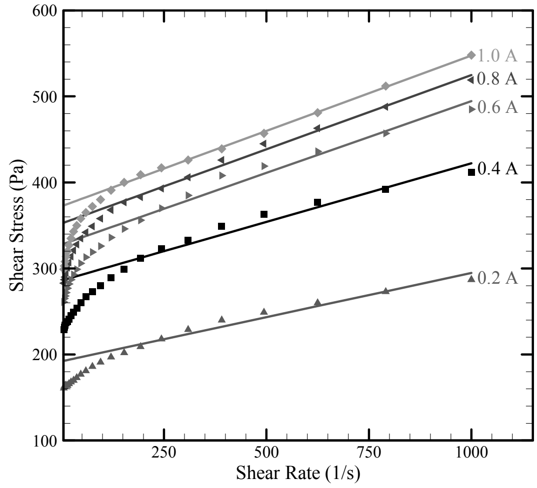

Fig. 10. Shear stress vs. shear rate at different magnetic fields (0.2-1 A) for the ferromagnetic nano-particle fluid (the BP model: curve-line, test: discrete marks).

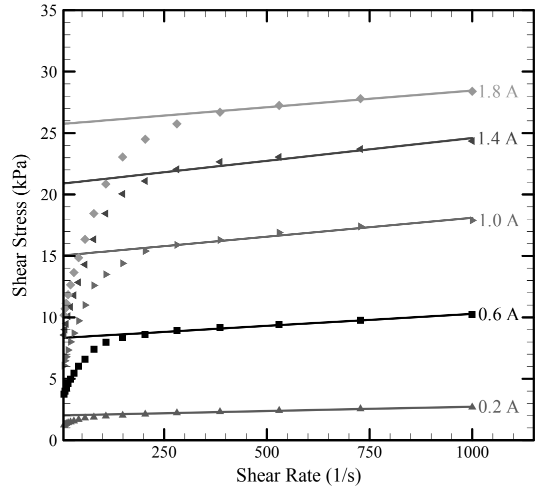

Fig. 11. Shear stress vs. the shear rate at different magnetic fields (0.2-1.8 A) for the MR fluid (the BP model: curve-line, test: discrete marks).

The rheology test results are compared with the BP model in Figs. 10 and 11. Similarly, a comparison of the rheology test results with the HB model is shown in Figs. 12 and 13. For the ferromagnetic nano-particle fluid, the BP model works properly in the post-yield regime for $\dot{\gamma} > 150$ 1/s; however, the HB model is suitable in both the pre-yield and post-yield regimes. For the MR fluid, the BP model is good over the entire range of magnetic fields, but for shear rates above a specific value. This value depends on the magnetic field. The

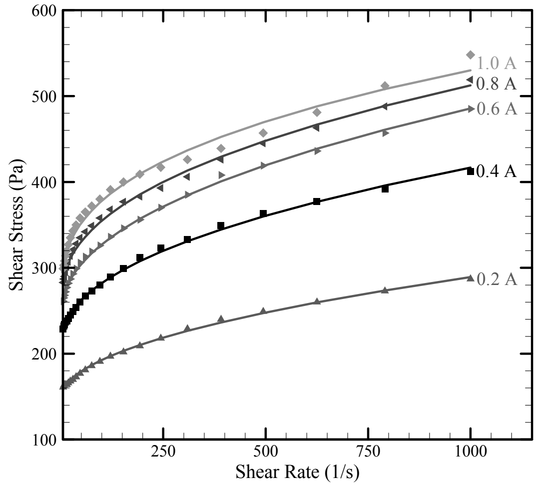

Fig. 12. Shear stress vs. the shear rate in different magnetic fields (0.2-1 A) for the ferromagnetic nano-particle fluid (the HB model: curve-line, test: discrete marks).

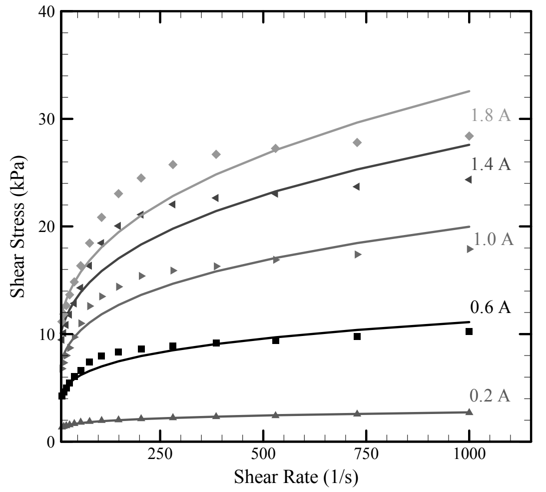

Fig. 13. Shear stress vs. the shear rate in different magnetic fields (0.2-1.8 A) for the MR fluid (the HB model: curve-line, test: discrete marks).

HB model is fine for all shear rates for $I < 0.6$ A.

Previous investigations have shown that yield stress is related to the field as follows [16]:

$$\tau_y \approx \sqrt{6}\phi\mu_0 M_s^{1/2} H^{3/2} \tag{14}$$

For low magnetic fields, Eq. (14) is given by [17]:

$$\tau_y \propto \phi\mu_0 H^2 \tag{15}$$

Our results also show that a quadratic polynomial closely fits the experimental values of the yield stress versus magnetic field (taking 'H' in kAm^{-1} or current 'I' in Amps). These variations can be represented accurately by the following equations:

$$\begin{aligned} \tau_y(\text{Pa}) &= -1.466\times10^3 I^2 + 1.81\times10^4 I - 1.799\times10^3 \\ \tau_y(\text{Pa}) &= -1.817\times10^{-2} H^2 + 84.83\ H - 1.074\times10^3 \end{aligned} \tag{16}$$

Similarly, quadratic polynomials corresponding to the behavior of the NMF material are obtained as:

$$\begin{aligned} \tau_y(\text{Pa}) &= -2.964\times10^2 I^2 + 5.67\times10^2 I + 95.5 \\ \tau_y(\text{Pa}) &= -7.016\times10^{-3} H^2 + 2.664\ H + 1.153\times10^2 \end{aligned} \tag{17}$$

5. Conclusions

Experiments were conducted to study the rheological behavior of selected smart EMR fluids in both pre-yield and post-yield regions. Typical viscoelastic and viscoplastic models were then employed to model the fluids' behavior. Two types of fluids including a ferromagnetic nano-particle fluid and a commercial MR fluid were fully examined. The rheological properties of the fluids in both frequency (oscillation mode) and time domains (rotational mode) were investigated using an MCR300 rheometer. Storage and loss moduli were measured in the oscillation mode while shear stress, shear rate, viscosity and torque were measured in the rotational mode.

Variations of storage and loss moduli vs. frequency were small at different magnetic fields for the ferromagnetic nano-particle fluid. Loss modulus was considerably smaller than storage modulus. The pre-yield behavior of the ferromagnetic nano-particle fluid was therefore modeled by Kelvin-Voigt model. Based on the results obtained in the rheology tests, the three-parameter fluid was used to model the pre-yield behavior of the MR fluid.

Time domain results were studied separately. Two viscoplastic models, Bingham-plastic (BP) and Herschel-Bulkley (HB) models, were adopted to model the rheological behavior of fluids in the time domain. The preferable model depended on the field strength and the shear rate. Both models were utilized to characterize the fluids' behavior.

The flow indices of the fluids are lower than unity (in HB model); the implication is that the fluids' behavior in the post-yield region is shear thinning. For the ferromagnetic nano-particle fluid, the BP model works well in the post-yield region. However, the HB model describes the material behavior adequately in both the pre-yield and post-yield regimes. For the MR fluid, the BP model is good over the entire range of the applied fields but for shear rates beyond certain values, which depend on the magnetic field. The HB model is fine for all shear rates at low magnetic fields. The models properly predicted the results observed in the experiments.

The models describing the dependence of the shear modulus and yield stress on the magnetic field were also investigated. Good conformity was obtained between the experimental values and the existing models that characterize these variations by quadratic polynomials.

Future attempts can be made to present a unique model incorporating both frequency and time domain results. Further investigations should also be conducted to extend the results obtained here for other MR fluids.

References

[1] A. Chaudhuri, N. M. Wereley, R. Radhakrishnan and S. B. Choi, Rheological parameter estimation for a ferrous nanoparticle-based magnetorheological fluid using genetic algorithms, *Journal of Intelligent Material Systems and Structures*, 17 (3) (2006) 261-269.

[2] M. R. Jolly and M. Nakano, Properties and applications of commercial controllable fluids. *In:Borgmann, H. (ed.). Actuator 1998. 6th International Conference on New Actuators*, Bremen 17-19 June 1998. Bremen: Messe Bremen GMBH. (1998) 411-416.

[3] F. Gandhi and W. A. Bullough, On the phenomenological modeling of electrorheological and magnetorheological fluid preyield behavior, *Journal of Intelligent Material Systems and Structures*, 16 (3) (2005) 237-248.

[4] R. A. Snyder, G. M. Kamath and N. M. Wereley, Characterization and analysis of magnetorheological damper behavior under sinusoidal loading, *AIAA Journal*, 39 (7) (2001) 1240-1253.

[5] R. Stanway, J. L. Sproston and A. K. El-Wahed, Applications of electro-rheological fluids in vibration control: a survey, *Smart Materials and Structures*, 5 (4) (1996) 464-482.

[6] N. D. Sims and N. M. Wereley, Modelling of smart fluid dampers, *Proceedings of the 2003 SPIE Conference on Smart Materials and Structures, Passive Damping and Isolation* SPIE Vol. 5052 (2003).

[7] N. D. Sims, N. J. Holmes and R. Stanway, A unified modeling and model updating procedure for electrorheological and magnetorheological vibration dampers, *Smart Materials and Structures*, 13 (1) (2004) 100-121.

[8] G. M. Kamath and N. M. Wereley, A nonlinear viscoelastic-plastic model for electrorheological fluids, *Smart Materials and Structures*, 6 (3) (1997) 351-359.

[9] G. M. Kamath and N. M. Wereley, Nonlinear viscoelastic-plastic mechanisms-based model of an electrorheological damper, *Journal of. Guidance, Control, and Dynamics*, 20 (6) (1997) 1125-1132.

[10] H. U. Oh and J. Onoda, An experimental study of a semiactive magneto-rheological fluid variable damper for vibration suppression of truss structures, *Smart Materials and Structures*, 11 (1) (2002) 156-162.

[11] J. Onoda, H. U. Oh and K. Minesugi, Semiactive vibration suppression with electrorheological-fluid dampers, *AIAA Journal*, 35 (12) (1997) 1844-1852.

[12] H. P. Gavin, Multi-duct ER dampers, *Journal of Intelligent Material Systems and Structures*, 12 (5) (2001) 353-366.

[13] G. M. Kamath, N. M. Wereley and M. R. Jolly, Characterization of magnetorheological helicopter lag dampers, *Journal-American Helicopter Society*, 44 (3) (1999) 234-248.

[14] M. Whittle, R. J. Atkin and W. A. Bullough, Fluid dynamic limitations on the performance of an electrorheological clutch, *Journal of Non-Newtonian Fluid Mechanics*, 57 (11) (1995) 61-81.

[15] D. R. Gamota and F. E. Filisko, Dynamic mechanical studies of electrorheological materials: Moderate frequencies, *Journal of Rheology*, 35 (3) (1991) 399-425.

[16] J. M. Ginder, L. C. Davis and L. D. Elie, Rheology of magnetorheological fluids: Models and measurements, *International Journal of Modern Physics*, 10 (23 & 24) (1996) 3293-3303.

[17] S. Genc and P. P. Phule, Rheology properties of magnetorheological fluids, *Smart Materials and Structures*, 11 (1) (2002) 140-146.

[18] Q. Sun, J. X. Zhou and L. Zhang, An adaptive beam model and dynamic characteristics of magnetorheological materials, *Journal of Sound and Vibration*, 261 (2) (2003) 465-481.

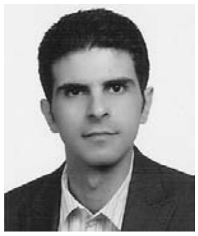

Nader Mohammadi received the BSc. in Mechanical Engineering, Tabriz University, Iran in 1998 and the MSc. And PhD. from Univ. of Tehran in 2000 and 20009. He is currently with the Department of Mech. Eng. , Azad University, Parand branch, Iran. His field has been noise control and industrial acoustics. He is currently working on sound transmission loss of ER materials.

M. J. Mahjoob (Mohammad Mahjoob Jahromi) received the BSc./MSc. from Univ. of Tehran in 1988 and the Ph.D. from University of Waterloo Canada in 1995, all in Mechanical Engineering. Since 1995, he has been with the School of Mechanical Engineering, University of Tehran, where he is now associate professor and director of NVA and Mechatronics center. His field of interest includes mechatronics, systems dynamics and control.